https://doi.org/10.17221/158/2020-CJFS

Transcriptomic analysis identifies differentially expressed genes in purple tender shoots and green mature leaves of Zijuan tea

*Bin Jiang[1], Lijiao Chen[1], Shuangmei Duan[2], Bo Nian[1], Kunyi Liu[1], Yan Ma[1], Ming Zhao[1,3,4]**

[1]*College of Tea Science, Yunnan Agricultural University, Kunming, China*
[2]*Dehong Extension Station of Tea Technology, Mangshi, China*
[3]*National & Local Joint Engineering Research Center on Germplasm Innovation & Utilization of Chinese Medicinal Materials in Southwestern China, Yunnan Agricultural University, Kunming, China*
[4]*Key Laboratory of Medicinal Plant Biology of Yunnan Province, Yunnan Agricultural University, Kunming, China*

**Corresponding author: zhaoming02292002@aliyun.com*

Citation: Jiang B., Chen L.J., Duan S.M., Nian B., Liu K.Y., Ma Y., Zhao M. (2022): Transcriptomic analysis identifies differentially expressed genes in purple tender shoots and green mature leaves of Zijuan tea. Czech J. Food Sci., 40: 210–220.

Abstract: Purple shoots of tea germplasm Zijuan (*Camellia sinensis* var. *asssamica*) have high anthocyanin content and gradually turn green with continued growth and development. To uncover the mechanism of this colour change, we performed transcriptome analysis to identify differentially expressed genes (DEGs). A total of 18 328 DEGs were identified in purple tender shoots of Zijuan (ZJP) compared with mature green leaves of Zijuan (ZJG). These included 85 DEGs associated with phenylpropanoid biosynthesis, 30 DEGs associated with flavonoid biosynthesis, and 3 DEGs involved in flavone and flavonol biosynthesis. We detected higher expression in ZJP than in ZJG of genes encoding the following key enzymes regulating anthocyanin biosynthesis and their corresponding metabolites: chalcone synthase (CHS), anthocyanidin synthase (ANS), anthocyanidin reductase (ANR), adenosine triphosphate (ATP)-binding cassette (ABC) transporters, bifunctional 3-dehydroquinate dehydratase (DHQ), chorismate mutase (CM), cinnamoyl-CoA reductase 1 (CCR), and cinnamyl alcohol dehydrogenase (CAD). In addition, upregulated expression of carbohydrate metabolism, glycolysis pathway, sucrose metabolism, and pyruvate metabolism suggested that glycolysis and upregulation of the sucrose synthase (SUS) gene may provide more intermediates as substrates for promoting anthocyanin accumulation in ZJP. Moreover, DEGs involved in anthocyanin biosynthesis, including phenylalanine ammonialyase (PAL), cinnamate acid 4-hydroxylase (C4H), chalcone isomerase (CHI), flavanone 3-hydroxylase (F3H), flavonol synthase (FLS), ANR, ANS, CHS, and flavonoid 3',5'-hydroxylase (F3'5'H) were significantly ($P < 0.01$) correlated with the contents of anthocyanin components such as cyanidin (Cy), delphinidin (Dp), peonidin (Pn), petunidin (Pt), and malvidin (Mv). The above results suggested that these upregulated DEGs may contribute to anthocyanin accumulation in ZJP and may play important roles in the colour changes in Zijuan tea. This research provided a foundation for clarifying the mechanisms underlying colour changes in Zijuan tea.

Keywords: colour change; transcriptome; anthocyanin metabolism; correlation; RNA-Seq

Supported by grants from the Yunnan Agricultural University Outstanding Scholar Project (Project No. 2015JY05), the National Natural Science Foundation of China (Projects No. 31160174, 31560221, and 31760225), the Cultivating Projects for Young Academic and Technical Leaders of Yunnan Province (Project No. 2017HB026), the Macau Science and Technology Development Fund (Project No. 009/2017/A1), the Earmarked Fund for China Agriculture Research System (Project No. CARS-19), and the Scientific Research Project of the Yibin Vocational and Technical College of China (Projects No. ZRKY21YB-06, ZRKY21YB-07).

https://doi.org/10.17221/158/2020-CJFS

In recent years, many researchers have studied anthocyanin-rich tea cultivars, such as Ziyan, Ziya, and Zijuan, for developing new products with abundant healthcare benefits for humans (Jiang et al. 2013; Joshi et al. 2015; Lai et al. 2016). Zijuan tea [*Camellia sinensis* var. *asssamica* (Masters) Kitamura] is excellent purple tea germplasm cultivated in China for its high anthocyanin content in immature shoots (0.58–6.16%) (Jiang et al. 2013). The purple leaves at the top of the stems gradually become green with leaf development, making them a good material for studying anthocyanin biosynthesis.

Plant anthocyanins are natural, water-soluble pigments that have been studied extensively owing to their notable antioxidation, tumour-suppression, and liver-protecting functions (Holton and Cornish 1995; Kang et al. 2015; Nabavi et al. 2018). Anthocyanins are produced by the typical biosynthetic pathway: phenylalanine → cinnamic acid → 4-coumaric acid → 4-coumaroyl-CoA → chalcone → naringenin → dihydrokaempferol → leucodelphinidin → delphinidin → delphinidin-3-glucoside → anthocyanins, and then stored in cell vacuoles where they exhibit different colours in the form of cyanine glycosides after glycosylation (Zhao et al. 2016). Ten genes related to anthocyanin metabolism in model plants, phenylalanine ammonialyase (PAL), cinnamate acid 4-hydroxylase (C4H), 4-coumarate-CoA ligase (4CL), chalcone synthase (CHS), chalcone isomerase (CHI), flavanone 3-hydroxylase (F3H), flavonoid 3',5'-hydroxylase (F3'5'H), flavonol synthase (FLS), dihydroflavonol 4-reductase (DFR), and anthocyanidin synthase (ANS), have been identified by transcriptome sequencing; these genes were confirmed to be essential for anthocyanin accumulation and play an important role in flavonoid metabolism (Wang et al. 2014, 2017; Zhao et al. 2014). In addition, key genes in *C. sinensis*, such as R2R3-MYB, CsAN1, and CsUGT72AM1, have been proven to regulate the accumulation of anthocyanins and flavonols in purple-leaf tea (Sun et al. 2016; He et al. 2018).

However, the regulatory mechanism of anthocyanin biosynthesis in purple leaves of Zijuan tea trees remains unclear. To explore the mechanism of purple shoot colouration in Zijuan, we conducted transcriptome analysis of the ZJP and ZJG. We identified differentially expressed genes (DEGs) in the anthocyanin biosynthesis and other metabolic pathways, including carbohydrate metabolism, shikimic acid pathway, and lignin biosynthesis, contributing to our understanding of anthocyanin biosynthesis in tea plants.

MATERIAL AND METHODS

Plant materials and high-performance liquid chromatography (HPLC) analysis of chemical compounds. Zijuan tea (*C. sinensis* var. Kitamura), an anthocyanin-rich tea cultivar, has long been grown in the Yunnan province of China and was classified as a variety for protection (No. 20050031) by the China State Forestry Administration in 2005 (Jiang et al. 2013). Fifteen Zijuan tea trees were chosen from the tea garden of the Tea Seed Multiplication Farm of Pu'er City, Yunnan Province, China. The trees were derived from a mother Zijuan tea tree [*C. sinensis* var. *assamica* (Masters) Kitamura] for which genetic identification had been performed and which were cultivated in the Germplasm Garden of Tea Research Institute, Yunnan Academy of Agricultural Sciences in Menghai, China. These 15 trees were divided into three groups (biological replicates) randomly, each group consisting of 5 trees. Purple tender shoots (ZJP) (one leaf and one bud) and green mature leaves (ZJG) of Zijuan tea trees with similar sizes and colours, and without disease-, insect-, or machinery-induced damage, were collected. A total of 35 ZJP and 35 ZJG samples from each group were harvested, respectively, in May 2018, and samples of the same type were pooled. All the samples were frozen quickly in liquid nitrogen and stored at –80 °C until use (89000 Series; Thermo Fisher Scientific, US). Contents of chemical compounds were detected by high-performance liquid chromatography (HPLC) analysis (1200 series; Agilent, US), as described previously by Zhao et al. (2015). Statistical analysis was performed using Prism 8 for Windows (GraphPad Software, US). One-way analysis of variance (ANOVA) was used for difference analysis, and $P < 0.05$ was considered to be significantly different. Results are expressed as mean ± standard deviation (SD) ($n = 3$).

Ribonucleic acid (RNA) extraction, complementary deoxyribonucleic acid (cDNA) library preparation, and sequencing. Total ribonucleic acid (RNA) was extracted using TRIzol (Vazyme Biotech, China) according to the manufacturer's instructions. The quality and concentration of extracted RNA were assessed using Agilent 2100 Bio-analyzer (Agilent, US) and NanoDrop ND-1000 spectrophotometer (NanoDrop, US), respectively. The construction of two complementary deoxyribonucleic acid (cDNA) libraries and transcriptome sequencing were performed by Guangzhou Gene Denovo Biotechnology Co., Ltd. (China). Briefly, the messenger ribonucleic acid (mRNA) was purified using oligo $(dT)_{18}$ (Thermo Fisher Scientific,

https://doi.org/10.17221/158/2020-CJFS

US) and was fragmented using NEBNext First Strand Synthesis Reaction Buffer (NEB, US). First strand cDNA was then synthesised using random hexamer primers, and the second strand was synthesised using ribonuclease H (RNaseH), DNA polymerase I, and deoxyribonucleotide triphosphates (dNTPs). After adenylation of the 3' end and purification of the cDNA library, polymerase chain reaction (PCR) was performed (QuantStudio 3; Thermo Fisher Scientific, US) using a high-fidelity thermostable DNA polymerase. Finally, the PCR products were purified using the AMPure XP system (Beckman Coulter, US), and library quality was assessed using Agilent 2100 Bioanalyzer (Agilent, US).

After clustering using a TruSeq PE Cluster Kit v3--cBot-HS (Illumina, US), the cDNA library generated was sequenced on an Illumina HiSeq^{TM} 2000 platform (Biomarker Biotech, China), and paired-end reads were generated. Three biological replicates were sequenced for each sample.

Functional annotation. Raw data were filtered by removing adapter sequences, low quality reads (those containing > 50% reads with quality value ≤ 20) and reads with > 5% unknown nucleotides, and clean reads were produced for further analysis. To categorise gene functions, all unigenes were aligned to the following public protein databases using Blastx (Altschul et al. 1997): nonredundant (Nr) database (Deng et al. 2006), Swiss--Prot (Magrane and Consortium 2011), Kyoto Encyclopaedia of Genes and Genomes (KEGG) (Minoru et al. 2007), and Cluster of Orthologous Groups of proteins (COG) (Tatusov et al. 2000). The best-aligning results were used to determine sequence directions. The proteins showing the highest sequence similarity to the given sequences identified in this study were retrieved and their functional annotations were determined. Gene ontology (GO) annotations were performed using the Blast2GO 5.0 program (Conesa et al. 2005). The Web Gene Ontology Annotation Plot (WEGO 2.0) software (Ye et al. 2006) was implemented to run the GO functional classifications for all sequences.

Differential expression analysis. Fragments per kilobase of transcript per million fragments (FPKM) were used to evaluate the expression of the genes (Florea et al. 2013). DEGs were screened according to the sequence-based differential gene detection method of Audic and Claverie (1997). Genes with expression levels showing $|\log_2 (\text{fold change})| > 1$ and false discovery rate (FDR) < 0.001 following Benjamini-Hochberg adjustment of *P*-value were considered as DEGs.

Quantitative reverse-transcription (qRT)-PCR verification analysis. The quantitative reverse-transcription (qRT)-PCR was performed to validate the reliability of RNA-sequencing (RNA-Seq) data. First strand cDNA was synthesised using a PrimeScript RT Reagent Kit with gDNA Eraser (Perfect Real Time) (Takara, Japan). qRT-PCR was performed in 20 µL reaction volumes containing 2 µL of 100 ng cDNA, 0.8 µL each of 10 µM forward and reverse primers, 0.4 µL ROX Reference Dye II, 10 µL TB Green Premix Ex Taq II (Tli RNaseH Plus) (Takara, Japan), and 6 µL ddH_2O. Primers for qRT-PCR of candidate DEGs are listed in Table S1 in electronic supplementary material (ESM; for the ESM see the electronic version). PCR was conducted using a QuantStudio 5 Real-Time PCR instrument (Applied Biosystems, US) with 40 cycles of 95 °C for 30 s, 95 °C for 5 s, and 60 °C for 30 s. All samples were analysed in three biological replicates. Chorionic somatomammotropin enhancer factor (CsEF) was used as a reference gene (Wu et al. 2016). Relative expression levels were calculated using the $2^{-\Delta\Delta CT}$ method (Iseli et al. 1999; Livak and Schmittgen 2001). Statistical analysis was performed using Microsoft Excel 2016 and GraphPad Prism 8.0 for Windows (GraphPad Software, US). One-way ANOVA was used for difference analysis, and $P < 0.05$ was considered to be significantly different.

RESULTS AND DISCUSSION

Chemical contents of tea leaves. Anthocyanin contents [delphinidin (Dp), cyanidin (Cy), pelargonidin (Pg), peonidin (Pn), petunidin (Pt), malvidin (Mv)] in ZJP were significantly higher than those in ZJG. This indicated that more anthocyanins are biosynthesised and accumulated in young tea leaves, which may partly account for the colour change in Zijuan shoots, consistent with previous studies (Li et al. 2017). There were discrepancies in the contents of catechins [(+)-catechin (C), (–)-epicatechin (EC), (–)-epigallocatechin (EGC), (–)-epicatechin-3-gallate (ECG), (–)-epigallocatechin-3-gallate (EGCG)], and flavonols [myricetin (Mc), quercetin (Qc), kaempferol (Kp)] (Figure 1 and Table S2 in ESM; for the ESM see the electronic version). These compounds share parts of the anthocyanin biosynthesis pathway, and anthocyanins are substrates for the biosynthesis of catechins in many plants (Guo and Wang 2010). Previous work in another purple tea showed consistent results (Lai et al. 2016; He et al. 2018). This may be related to the different expression of genes in the anthocyanin metabolic pathway (Wang et al. 2017). Furthermore, anthocyanins are considered as functional substances in anti-ageing, suppressing cancer tumours, reducing

https://doi.org/10.17221/158/2020-CJFS

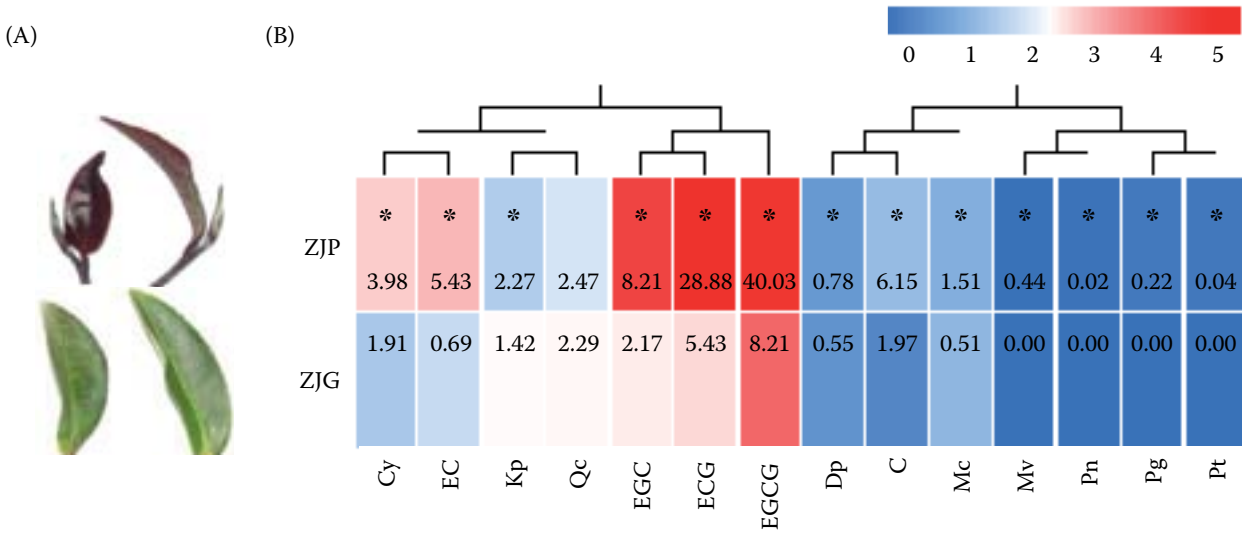

Figure 1. Comparison of chemical compound contents between ZJP and ZJG: (A) experimental materials, (B) heatmap diagram showing disparity in catechin, anthocyanin, and flavonol contents

*Significant difference ($P < 0.05$); ZJP – purple tender shoots of Zijuan; ZJG – mature green leaves of Zijuan; Cy – cyanidin; EC – (–)-epicatechin; Kp – kaempferol; Qc – quercetin; EGC – (–)-epigallocatechin; ECG – (–)-epicatechin-3-gallate; EGCG – (–)-epigallocatechin-3-gallate; Dp – delphinidin; C – catechin; Mc – myricetin; Mv – malvidin; Pn – peonidin; Pg – pelargonidin; Pt – petunidin; the heatmap was constructed based on $\log_2$ (chemical compound content); data are presented as the mean ($n = 3$)

blood lipid levels, protecting the liver, and performing other physiological effects in humans (Kerio et al. 2013; Forester et al. 2014). Thus, ZJP should be harvested during tea processing, and this tea product should be purchased in the tea market.

DEG identification and enrichment analysis. To elucidate the molecular mechanism underlying purple colour formation, we performed RNA-Seq analysis using the Illumina platform. Each library for ZJP and ZJG produced 25 979 110 to 30 039 234 and 22 151 300 to 25 095 360 total raw reads, respectively, following cleaning and quality checks. Q20 values (proportion of nucleotides with read quality values larger than 20) were over 93.92%, and guanine-cytosine (GC) percentages were 43.98% to 44.31% for ZJP and 43.27% to 44.18% for ZJG (Table 1). These data showed that the RNA-Seq quality was good and the data could be used for further analysis.

Gene expression is closely related to the concentration of total catechins and anthocyanins at various stages of leaf development (Li et al. 2017). In our transcriptome, we identified 18 328 DEGs between ZJP and ZJG libraries based on the reads per kilo base of transcript per million mapped reads (RPKM) method. Of these, 12 371 were upregulated and 5 975 were downregulated in ZJP compared with ZJG (Figure S1 and Table S3 in ESM; for the ESM see the electronic version). After matching the sequences to those available in public protein databases, 36 621 unigenes were annotated, with 36 451, 24 260, 10 674, and 9 155 matching annotated genes in the Nr, Swiss-Prot, COG and KEGG databases, respectively. GO analysis revealed that 18 328, 12 052, and 14 093 DEGs were enriched to categories of 31 biological processes (BP), 14 cellular components (CC), and 24 molecular functions (MF), respectively. The terms 'metabolic process', 'cellular process', and 'single-organism process' were the dominant categories enriched among BP; 'cell', 'cell part', and 'organelle' were highly represented categories among CC. A large proportion of genes were enriched in 'metabolic process', 'catalytic activity', and 'cellular process' categories for MF (Table S4 in ESM; for the ESM see the electronic version).

We mapped all DEGs to the KEGG database, and 2 851 DEGs were enriched to 115 pathways (Table S4 in ESM; for the ESM see the electronic version). Most of these DEGs were enriched in 'phenylpropanoid biosynthesis' (up-/down-regulated unigenes in ZJP compared with ZJG: 73/12), 'flavonoid biosynthesis' (28/2), 'plant hormone signal transduction' (82/38), and 'biosynthesis of secondary metabolites' (374/29), followed by other pathways such as 'metabolic pathways' (504/256) and 'nitrogen metabolism' (27/9); 'cyanoamino acid metabolism' (20/5) and 'tyrosine metabolism' (12/5) showed the lowest enrichment. To uncover the

https://doi.org/10.17221/158/2020-CJFS

Table 1. Transcriptome quality for ZJP and ZJG

Samples	Total reads	Mapped reads		GC contents	Q20
		n	(%)	(%)	(%)
ZJP-1	27 251 108	15 209 486	55.81	44.31	94.13
ZJP-2	25 979 110	14 240 572	54.82	43.98	95.32
ZJP-3	30 039 234	16 702 336	55.60	44.26	94.56
ZJG-1	25 095 360	13 871 952	55.28	43.76	95.18
ZJG-2	22 151 300	12 373 421	55.86	44.18	94.84
ZJG-3	22 515 748	12 737 633	56.57	43.27	93.92

ZJP – purple tender shoots of Zijuan; ZJG – mature green leaves of Zijuan; GC – guanine-cytosine; Q20 – proportion of nucleotides with read quality values larger than 20

mechanism behind the colour change, we paid most attention to the metabolic pathways, especially those involving flavonoid, phenylpropanoid, flavone, and flavonol biosynthesis, anthocyanin transportation, and carbohydrate metabolism (Li et al. 2017). This indicated that increased anthocyanin content in ZJP was probably correlated with high expression levels of related genes in each pathway.

DEGs involved in anthocyanin biosynthesis and transportation pathways. Anthocyanins are water-soluble, natural pigments existing widely in plants and belong to flavonoids. Anthocyanin biosynthesis is a subpathway of flavonoid biosynthesis in phenylpropanoid metabolism, which is a complex secondary metabolic network (Guo and Wang 2010). We identified 14 enzymes related to anthocyanin metabolism using KEGG function annotation and comparison with the SwissProt database, and these are regulated by the expression of 48 unigenes (Figure 2 and Table S5 in ESM; for the ESM see the electronic version). In the phenylpropanoid biosynthesis pathway, 18 upregulated unigenes encoded PAL, seven upregulated unigenes encoded 4CL, and two upregulated unigenes encoded shikimate O-hydroxycinnamoyltransferase (HCT) and trans-cinnamate 4-monooxygenase (CYP73A), respectively. Only one unigene encoded uridine diphosphate (UDP)-glycosyltransferase (UGT72E) (Figure 2A). The catalytic activity of these enzymes provides additional substrates such as 4-coumaroyl-CoA for flavonoid biosynthesis, laying the foundation for anthocyanin accumulation (Li et al. 2017). Paralogous 'purple colour' genes, including CHS, CHI, flavonoid 3'-hydroxylase (F3'H), and ANS, were upregulated in ZJP (Tanaka et al. 2010; Clark and Verwoerd 2011) (Figure 2B). For the flavonoid biosynthesis pathway, two upregulated unigenes encoded CYP73A, HCT, FLS and anthocyanidin reductase (ANR), respectively. One upregulated unigene encoded CHI, four upregulated unigenes encoded CHS, and one up- and one down-regulated unigene encoded F3H. In the flavone and flavonol biosynthesis pathway, two upregulated unigenes encoded flavonoid 3'5'-hydroxylase (F3'5'H) and one upregulated unigene encoded flavonoid 3'-monooxygenase (CYP75B1) (Figure 2C). In anthocyanin transportation, two upregulated unigenes encoded adenosine triphosphate (ATP)-binding cassette (ABC) (Table S5 in ESM; for the ESM see the electronic version). Previous studies indicate that PAL, C4H, 4CL, CHS, DFR, and ANS are critical enzymes for anthocyanin biosynthesis (Hu et al. 2010; Zhao et al. 2016). CHS catalyses the first step reaction of anthocyanin biosynthesis (Koes et al. 1989); if CHS activity is absent, anthocyanin glycosides and other flavonoids will be absent, resulting in white flower mutants (Hoshino et al. 2009). Overexpression of ANS increases the accumulation of flavonoids and anthocyanidins in rice plants, with the seed coat showing a purple-red colour (Reddy et al. 2007). Two upregulated ABC genes in ZJP might also contribute to increased accumulation and transport of anthocyanins compared with ZJG (Li et al. 2017).

DEGs involved in carbohydrate metabolism, phenylalanine biosynthesis, and the branched pathway of anthocyanin biosynthesis. Anthocyanin formation is stimulated greatly by carbohydrates such as glucose and sucrose (Kim et al. 2006). Phenylalanine is a primary substrate in anthocyanin biosynthesis, and phenylalanine biosynthesis plays an important role in anthocyanin accumulation in tea plant cells (Wang et al. 2017). In our study, the majority of genes related to carbohydrate metabolism and the phenylalanine pathway were upregulated in ZJP. Five upregulated unigenes encoded sucrose synthase (SUS), two upregulated unigenes encoded phosphoglycerate mutase (PGmu), nine upregulated unigenes encoded acetyl-coenzyme A carboxylase (ACCase), and two upregulated unigenes encoded chorismate mutase (CM), while hexokinase (HXK), pyruvate

https://doi.org/10.17221/158/2020-CJFS

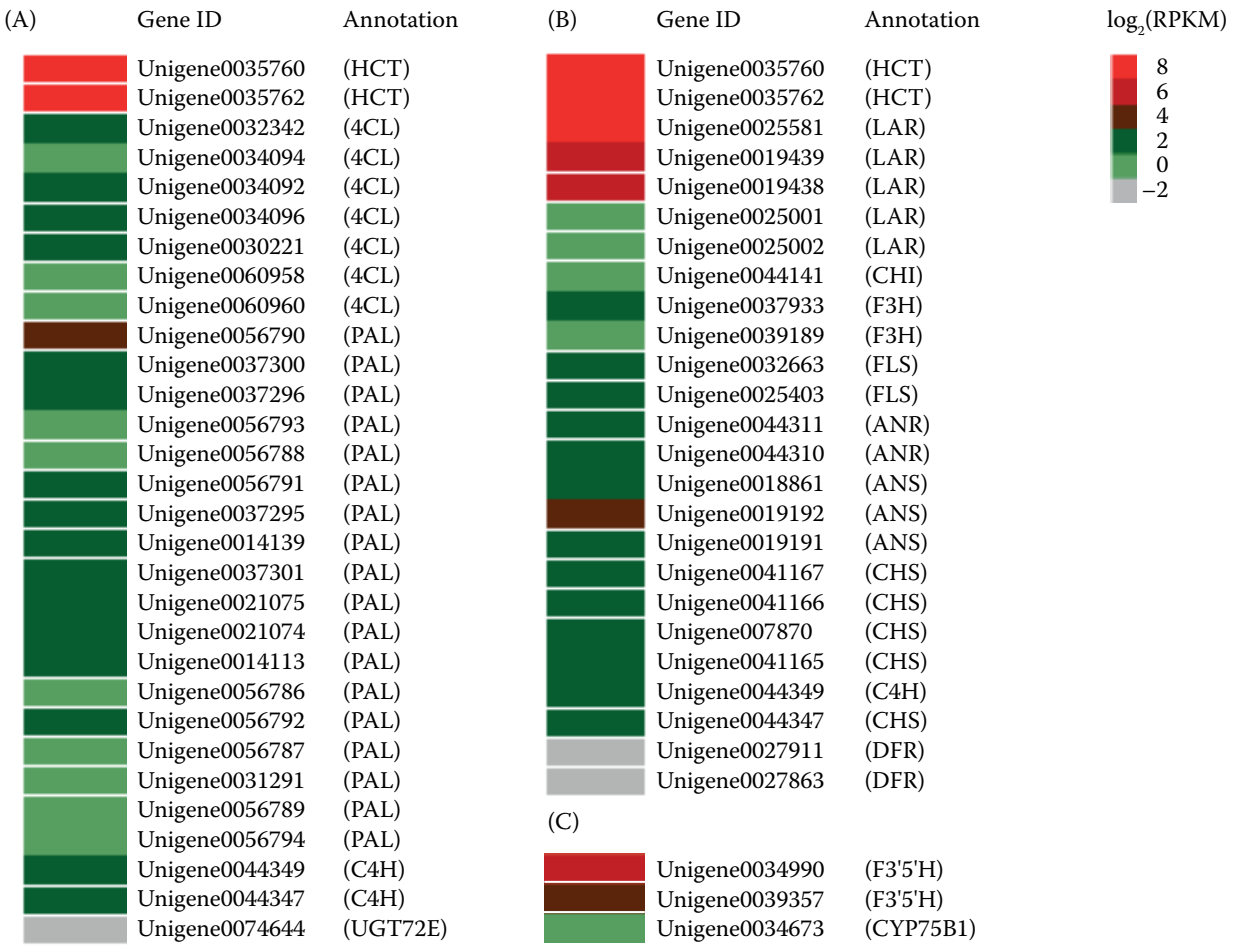

Figure 2. Heatmap diagram of expression patterns for DEGs involved in the anthocyanin biosynthesis pathway, including (A) phenylpropanoid, (B) flavonoid, and (C) flavone and flavonol biosynthesis pathways

DEGs – differentially expressed genes; HCT – shikimate O-hydroxycinnamoyltransferase; 4CL – 4-coumarate-CoA ligase; PAL – phenylalanine ammonialyase; C4H – cinnamate acid 4-hydroxylase; UGT72E – uridine diphosphate (UDP)--glycosyltransferase; LAR – leucoanthocyanidin reductase; CHI – chalcone isomerase; F3H – flavanone 3-hydroxylase; FLS – flavonol synthase; ANR – anthocyanidin reductase; ANS – anthocyanidin synthase; CHS – chalcone synthase; DFR – dihydroflavonol 4-reductase; F3'5'H – flavonoid 3',5'-hydroxylase; CYP75B1 – flavonoid 3'-monooxygenase; RPKM – reads per kilo base of transcript per million mapped reads; heatmaps were constructed based on $\log_2$ [RPKM of purple tender shoots/mature green leaves of Zijuan (ZJP/ZJG)]; red and grey colours indicate up- and down-regulated genes in the ZJP library compared with the ZJG library, respectively

kinase (PK), pyruvate dehydrogenase (PDH) and 3-dehydroquinate dehydratase (DHQ) were encoded by one upregulated unigene, respectively. We used these findings and analysis to reconstruct the molecular regulatory network of anthocyanin metabolism in ZJP of Zijuan tea (Figure 3).

Sucrose initiates signalling pathways leading to altered gene expression and physiological adaptation and induces expression of MYB75/PAP1 (Teng et al. 2005), which activates the expression of anthocyanin biosynthesis genes (Solfanelli et al. 2006). Moreover, SUS also generates sucrose biosynthesis by catalysing the conversion of UDP-glucose and fructose into sucrose (Baroja-Fernandez et al. 2012). Anthocyanidin 3-O-glucosyltransferase (UFGT) catalyses the transfer of a glucosyl moiety from UDP-glucose to Cy, indicating that SUS may play a vital role in anthocyanin biosynthesis by providing UDP-glucose and hexoses. A previous study indicates that upregulated genes related to anthocyanin biosynthesis include PGmu and PK in the glycolysis pathway, implying that glycolysis may provide more intermediates as substrates for promoting anthocyanin accumulation (Voll et al. 2009). We identified one upregulated unigene encoding HXK. In the glycolysis pathway, HXK catalyses the phosphorylation of hexoses to form hexose 6-phosphates,

https://doi.org/10.17221/158/2020-CJFS

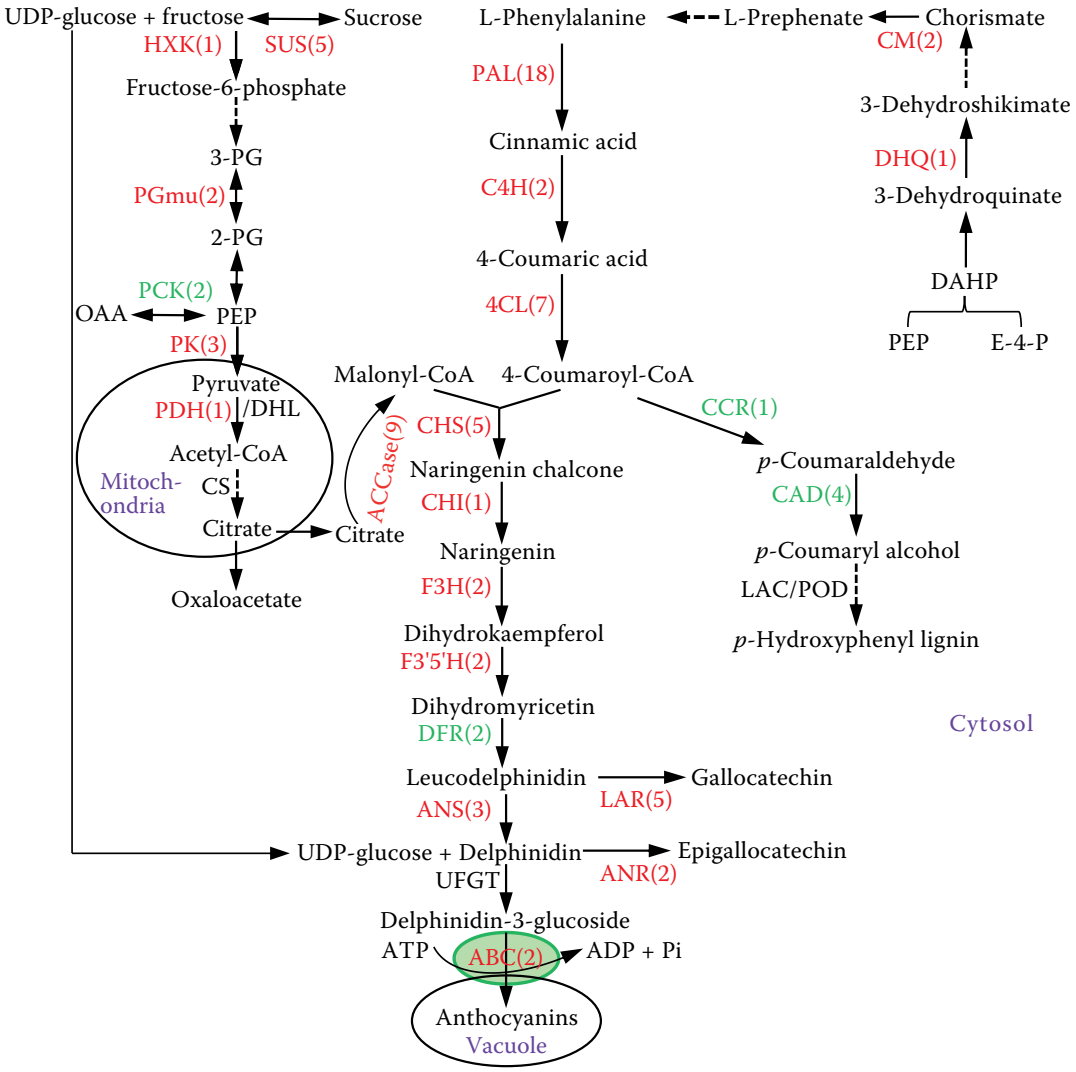

Figure 3. Molecular regulatory network of anthocyanin metabolism in Zijuan tea

UDP – uridine diphosphate; HXK – hexokinase; SUS – sucrose synthase; PG – phosphoglyceric acid; PGmu – phosphoglycerate mutase; PCK – phosphoenolpyruvate carboxykinase; PK – pyruvate kinase; PEP – phosphoenolpyruvate; OAA – oxaloacetic acid; PDH – pyruvate dehydrogenase; DHL – dehydroleucodine; CS – 2-chlorobenzalmalononitrile; ACCase – acetyl-coenzyme A carboxylase; PAL – phenylalanine ammonialyase; C4H – cinnamate acid 4-hydroxylase; 4CL – 4-coumarate-CoA ligase; CCR – cinnamoyl-CoA reductase 1; CAD – cinnamyl alcohol dehydrogenase; CHS – chalcone synthase; CHI – chalcone synthase; F3H – flavanone 3-hydroxylase; F3'5'H – flavonoid 3',5'-hydroxylase; DFR – dihydroflavonol 4-reductase; ANS – anthocyanidin synthase; LAR – leucoanthocyanidin reductase; ANR – anthocyanidin reductase; UFGT – anthocyanidin 3-O-glucosyltransferase; ABC – adenosine triphosphate (ATP)-binding cassette; ADP +Pi – adenosine diphosphate after removing one of the phosphates (Pi); CM – chorismate mutase; DHQ – 3-dehydroquinate dehydratase; LAC – laccase; POD – peroxidase; DAHP – 3-deoxy-D-arabinoheptulosonate-7-phosphate; PEP – phosphoenolpyruvate; E-4-P – erythrose 4-phosphate; the network integrates 21 differentially expressed genes (DEGs) indicated in red (upregulated at purple leaf stage) or green (downregulated at purple leaf stage), respectively; numbers in brackets indicate the number of DEGs

which are involved in sucrose signal transduction, promoting anthocyanin accumulation.

The PDH complex comprising dihydrolipoate trans-acetylase, PDH, and dehydroleucodine (DHL) plays a critical role in the utilisation of pyruvate, leading to its conversion to acetyl-coenzyme A (acetyl-CoA) for energy production or biosynthetic processes (Li et al. 2017). Moreover, in the plant cytosol, ACCase catalyses the carboxylation of cytosolic acetyl-CoA to malonyl-CoA, which can be incorporated into anthocyanin biosynthesis through CHS (Sasaki and Nagano 2004; Zheng and Tian 2006; Cui et al. 2017); ACCase is a key enzyme

https://doi.org/10.17221/158/2020-CJFS

in the production of malonyl-CoA during anthocyanin biosynthesis (Cui et al. 2017). In the phenylalanine biosynthetic pathway of tea, DHQ and CM showed distinctly higher abundance in ZJP than ZJG, providing a sufficient phenylalanine substrate for anthocyanin synthesis. DHQ and CM are key enzymes that catalyse the conversion of phosphoenolpyruvate and erythritol 4-phosphate to phenylalanine (Knaggs et al. 2003). DHQ catalyses 3-dehydroquinic to shikimic acid. The conversion of chorismic acid, a major substrate in phenylalanine biosynthesis, to prephenate is catalysed by CM. Thus, the upregulation of genes encoding these enzymes could provide a sufficient substrate for anthocyanin biosynthesis and promote anthocyanin accumulation in the ZJP (Wang et al. 2017).

Intermediates of the anthocyanin biosynthetic pathway can be used for the biosynthesis of other secondary metabolites. For example, the conversion of 4-coumaric acyl-CoA to *p*-coumaraldehyde is catalysed by cinnamoyl-CoA reductase 1 (CCR), and cinnamyl alcohol dehydrogenase (CAD) can then catalyse *p*-coumaraldehyde to *p*-coumaryl alcohol; these are two key enzymes regulating the lignin biosynthesis pathway (Leple et al. 2007). Thus, in this study, lower abundances of CCR and CAD resulted in an increased flow of intermediates into the anthocyanin biosynthesis pathway. This suggested that more 4-coumaric acyl-CoA flowed into anthocyanin biosynthesis when lignin biosynthesis was suppressed in ZJP.

Validation by qRT-PCR. We randomly selected 10 DEGs for qRT-PCR to validate their expression levels during the maturation process of Zijuan tea trees. Figure 4 shows that the expression levels of these genes, namely, PAL, 4CL, CHS, CHI, F3H, F3'5'H, leucoanthocyanidin reductase (LAR), ANS, and ANR, in ZJP were greater than those in ZJG. However, the expression levels of DFR were markedly lower than those in ZJG ($P < 0.05$). The results from qRT-PCR analysis were consistent with those from the Illumina sequencing data (Table S6 in ESM; for the ESM see the electronic version), which validated the expression profile of the differentially expressed unigenes and confirmed the reliability of our transcriptome sequencing analysis.

Correlation network analysis. In order to reveal the relationship between DEGs and chemical compounds, we filtered DEGs with FPKM > 50 and calculated Spearman's correlation coefficients (ρ) between these DEGs and chemical compounds; |ρ| greater than 0.6 are shown using a network diagram (Figure 5). As shown in Figure 5, all of the DEGs were positively correlated with chemical compounds. In particular, DEGs involved in anthocyanin biosynthesis, including PAL, C4H, CHI,

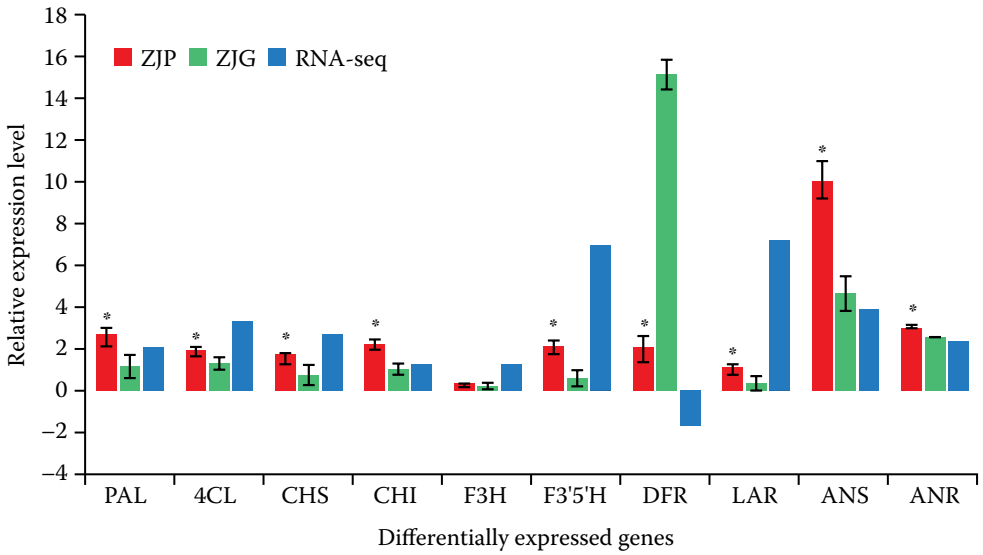

Figure 4. Comparison of RNA-Seq data and qRT-PCR verification of DEGs

RNA-Seq – ribonucleic acid-sequencing; qRT-PCR – quantitative reverse-transcription-polymerase chain reaction; DEG – differentially expressed genes; ZJP – purple tender shoots of Zijuan; ZJG – mature green leaves of Zijuan; PAL – phenylalanine ammonialyase; 4CL – 4-coumarate-CoA ligase; CHS – chalcone synthase; CHI – chalcone synthase; F3H – flavanone 3-hydroxylase; F3'5'H – flavonoid 3',5'-hydroxylase; DFR – dihydroflavonol 4-reductase; LAR – leucoanthocyanidin reductase; ANS – anthocyanidin synthase; ANR – anthocyanidin reductase; red and green bars represent expression of DEGs based on RT-PCR data; blue bars represent the fold change of DEG expression levels based on RNA-Seq data; RT-PCR data are presented as the mean ± standard deviation (SD) ($n = 3$)

https://doi.org/10.17221/158/2020-CJFS

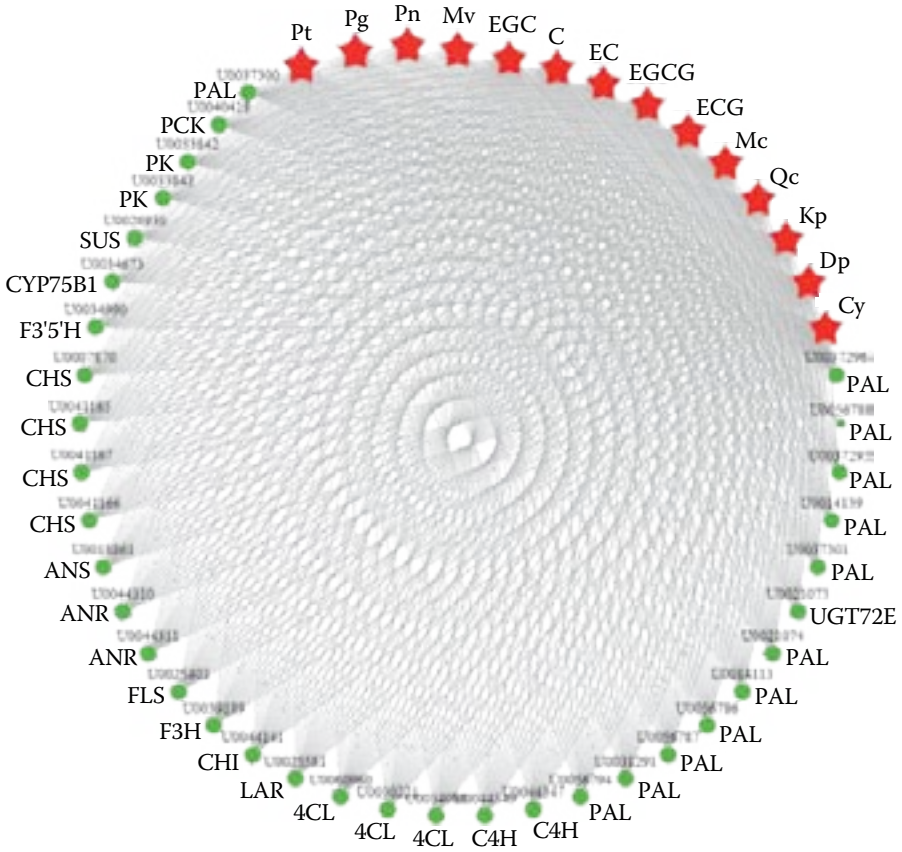

Figure 5. Correlation analysis between DEGs and chemical compounds

U – unigene; PAL – phenylalanine ammonialyase; UGT72E – uridine diphosphate (UDP)-glycosyltransferase; C4H – cinnamate acid 4-hydroxylase; 4CL – 4-coumarate-CoA ligase; LAR – leucoanthocyanidin reductase; CHI – chalcone synthase; F3H – flavanone 3-hydroxylase; FLS – flavonol synthase; ANR – anthocyanidin reductase; ANS – anthocyanidin synthase; CHS – chalcone synthase; F3'5'H – flavonoid 3',5'-hydroxylase; CYP75B1 – flavonoid 3'-monooxygenase; SUS – sucrose synthase; PK – pyruvate kinase; PCK – phosphoenolpyruvate carboxykinase; Pt – petunidin; Pg – pelargonidin; Pn – peonidin; Mv – malvidin; EGC – (–)-epigallocatechin; C – (+)-catechin; EC – (–)-epicatechin; EGCG – (–)-epigallocatechin-3-gallate; ECG – (–)-epicatechin-3-gallate; Mc – myricetin; Qc – quercetin; Kp – kaempferol; Dp – delphinidin; Cy – cyanidin; a connection (i.e. edge) indicates a positive (grey line) correlation, with the absolute value of Spearman's correlation coefficient more than 0.6

F3H, FLS, ANR, ANS, CHS, and F3'5'H, were significantly ($P < 0.01$) correlated with the contents of anthocyanin components such as Cy, Dp, Pn, Pt, and Mv. Interestingly, in ZJP, these DEGs were upregulated and anthocyanin components were significantly higher than in ZJG. The above results suggested that the upregulation of genes involved in anthocyanin biosynthesis may contribute to anthocyanin accumulation in ZJP and plays important roles in the colour changes in Zijuan tea trees.

CONCLUSION

We employed RNA-Seq technology to systematically identify DEGs at the transcriptome level in leaves of Zijuan tea at the purple and green stages. We found that most genes participating in the processes of anthocyanin biosynthesis and their transportation were upregulated in ZJP. Genes associated with carbohydrate metabolism and phenylalanine pathway were also upregulated, while genes participating in the branched pathway in anthocyanin biosynthesis were downregulated in ZJP. DEGs involved in anthocyanin biosynthesis and accumulation were confirmed by qRT-PCR. Moreover, DEGs involved in anthocyanin biosynthesis, including PAL, C4H, CHI, F3H, FLS, ANR, ANS, CHS and F3'5'H, were significantly correlated with the contents of anthocyanin components. This is the first time to our knowledge that the effects of carbohydrate metabolism, the shikimic acid pathway, and lignin biosynthesis on anthocyanin biosynthesis, and the an-

https://doi.org/10.17221/158/2020-CJFS

thocyanin biosynthesis regulatory network have been dissected in Zijuan tea. The data generated in this study will be a valuable source for further molecular studies of anthocyanin biosynthesis in purple tea.

REFERENCES

Altschul S.F., Madden T.L., Schaffer A.A. (1997): Gapped BLAST and PSI-BLAST: A new generation of protein database search programs. Nucleic Acids Research, 25: 3389–402.

Audic S., Claverie J.M. (1997): The significance of digital gene expression profiles. Genome Research, 7: 986–995.

Baroja-Fernandez E., Munoz F.J., Li J., Bahaji A., Almagro G., Montero M. (2012): Sucrose synthase activity in the sus1/sus2/sus3/sus4 Arabidopsis mutant is sufficient to support normal cellulose and starch production. Proceedings of the National Academy of Sciences, 109: 321–326.

Clark S.T., Verwoerd W.S. (2011): A systems approach to identifying correlated gene targets for the loss of colour pigmentation in plants. BMC Bioinformatics, 12: 343.

Conesa A., Gotz S., Garcia-Gomez J.M., Terol J., Talon M., Robles M. (2005): Blast2GO: A universal tool for annotation, visualization and analysis in functional genomics research. Bioinformatics, 21: 3674–3676.

Cui Y.P., Zhao Y.P., Wang Y.M., Liu Z.J., Babar I., Hua J.P. (2017): Genome-wide identification and expression analysis of the biotin carboxyl carrier subunits of heteromeric acetyl-CoA carboxylase in *Gossypium*. Frontiers in Plant Science, 8: 624.

Deng Y.Y., Li J.Q., Wu S.F., Zhu Y.P., He F.C. (2006): Integrated nr database in protein annotation system and its localization. Computer Engineering, 32: 71–72.

Florea L., Song L., Salzberg S.L. (2013): Thousands of exon skipping events differentiate among splicing patterns in sixteen human tissues. F1000Research, 2: 188.

Forester S.C., Choy Y.Y., Waterhouse A.L., Oteiza P.I. (2014): The anthocyanin metabolites gallic acid, 3-o-methylgallic acid, and 2,4,6-trihydroxybenzaldehyde decrease human colon cancer cell viability by regulating pro-oncogenic signals. Molecular Carcinogenesis, 53: 432–439.

Guo J., Wang M.H. (2010): Ultraviolet A-specific induction of anthocyanin biosynthesis and PAL expression in tomato (*Solanum lycopersicum* L.). Plant Growth Regulation, 62: 1–8.

Holton T.A., Cornish E.C. (1995): Genetics and biochemistry of anthocyanin biosynthesis. Plant Cell, 7: 1071–1083.

He X., Zhao X., Gao L., Shi X., Dai X., Liu Y. (2018): Isolation and characterization of key genes that promote flavonoid accumulation in purple-leaf tea (*Camellia sinensis* L.). Scientific Reports, 8: 130.

Hu Y., Gai Y., Yin L., Wang X., Feng C., Feng L. (2010): Crystal structures of a *Populus tomentosa* 4-coumarate: CoA ligase shed light on its enzymatic mechanisms. The Plant Cell, 22: 3093–3104.

Hoshino A., Park K., Iida S. (2009): Identification of r mutations conferring white flowers in the Japanese morning glory (*Ipomoea nil*). Journal of Plant Research, 122: 223–223.

Iseli C., Jongeneel C.V., Bucher P. (1999): ESTScan: A program for detecting, evaluating, and reconstructing potential coding regions in EST sequences. In: International Conference on Intelligent Systems for Molecular Biology, Heidelberg, Germany, Aug 6–10, 1999: 138–148.

Jiang L., Shen X., Shoji T., Kanda T., Zhao L. (2013): Characterization and activity of anthocyanins in Zijuan tea (*Camellia sinensis* var. Kitamura). Journal of Agricultural and Food Chemistry, 61: 3306–3310.

Joshi R., Rana A., Gulati A. (2015): Studies on quality of orthodox teas made from anthocyanin-rich tea clones growing in Kangra valley, India. Food Chemistry, 176: 357–366.

Kang W., Liyuan W., Chengcai Z., Liyun W., Hailin L., Fen Z. (2015): Transcriptome analysis reveals key flavonoid 3'-hydroxylase and flavonoid 3',5'-hydroxylase genes in affecting the ratio of dihydroxylated to trihydroxylated catechins in *Camellia sinensis*. PLoS ONE, 10: e0137925.

Kerio L.C., Wachira F.N., Wanyoko J.K., Rotich M.K. (2013): Total polyphenols, catechin profiles and antioxidant activity of tea products from purple leaf coloured purple tea cultivars. Food Chemistry, 136: 1405–1413.

Koes R.E., Spelt C.E., van den Elzen P.J.M., Mol J.N.M. (1989): Cloning and molecular characterization of the chalcone synthase multigene family of *Petunia hybrida*. Gene, 81: 245–257.

Kim J.S., Lee B.H., Kim S.H., Oh K.H., Cho K.Y. (2006): Responses to environmental and chemical signals for anthocyanin biosynthesis in non-chlorophyllous corn (*Zea mays* L.) leaf. Journal of Plant Biology, 49: 16–25.

Knaggs A.R. (2003): The biosynthesis of shikimate metabolites. ChemInform, 34: 119–136.

Lai Y.S., Li S., Tang Q., Li H.X., Chen S.X. (2016): The dark--purple tea cultivar 'Ziyan' accumulates a large amount of delphinidin. Journal of Agricultural and Food Chemistry, 64: 2719–2726.

Livak K.J., Schmittgen T.D. (2001): Analysis of relative gene expression data using real-time quantitative PCR and the $2^{-\Delta\Delta CT}$ method. Methods, 4: 402–408.

Li J., Lv X.J., Wang L.X., Qiu Z.M., Song X.M., Lin J.K., Chen W. (2017): Transcriptome analysis reveals the accumulation mechanism of anthocyanins in 'Zijuan' tea (*Camellia sinensis* var. *asssamic*a (Masters) Kitamura) leaves. Plant Growth Regulation, 81: 51–61.

https://doi.org/10.17221/158/2020-CJFS

Leple J.C., Dauwe R., Morreel K., Veronique S., Boerjan W. (2007): Downregulation of cinnamoyl-coenzyme A reductase in poplar: Multiple-level phenotyping reveals effects on cell wall polymer metabolism and structure. The Plant Cell, 19: 3669–3691.

Magrane M., Consortium U. (2011): UniProt Knowledgebase: A hub of integrated protein data. Database: The Journal of Biological Databases and Curation, 2011: bar009.

Minoru K., Michihiro A., Susumu G., Masahiro H., Mika H., Masumi I. (2007): Kegg for linking genomes to life and the environment. Nucleic Acids Research, 36: D480–D484.

Nabavi S.M., Šamec D., Tomczyk M., Luigi M., Daniela R., Solomon H., Ipek S., Luca R., Jianbo X., Francesca G., Maurizio B., Eduardo S.S., Seyed F.N., Bahman Y., Philippe J., Suowen X., Samira S. (2018): Flavonoid biosynthetic pathways in plants: Versatile targets for metabolic engineering. Biotechnology Advances, 38: 107316.

Reddy A.M., Reddy V.S., Scheffler B.E., Wienand U., Reddy A.R. (2007): Novel transgenic rice overexpressing anthocyanidin synthase accumulates a mixture of flavonoids leading to an increased antioxidant potential. Metabolic Engineering, 9: 95–111.

Sun B., Zhu Z., Cao P., Chen H., Chen C., Zhou X. (2016): Purple foliage coloration in tea (*Camellia sinensis* L.) arises from activation of the r2r3-myb transcription factor csan1. Scientific Reports, 6: 32534.

Solfanelli C., Poggi A., Loreti E., Alpi A., Perata P. (2006): Sucrose-specific induction of the anthocyanin biosynthetic pathway in *Arabidopsis*. Plant Physiology, 140: 637–646.

Sasaki Y., Nagano Y. (2004): Plant acetyl-CoA carboxylase: Structure, biosynthesis, regulation, and gene manipulation for plant breeding. Journal of the Agricultural Chemical Society of Japan, 68: 1175–1184.

Tatusov R.L., Galperin M.Y., Natale D.A., Koonin E.V. (2000): The COG database: A tool for genome-scale analysis of protein functions and evolution. Nucleic Acids Research, 28: 33–36.

Tanaka Y., Brugliera F., Kalc G., Senior M., Chandler S. (2010): Flower color modification by engineering of the flavonoid biosynthetic pathway: Practical perspectives. Bioscience, Biotechnology, and Biochemistry, 74: 1760–1769.

Teng S., Keurentjes J., Leónie B.T., Smeekens K.S. (2005): Sucrose-specific induction of anthocyanin biosynthesis in *Arabidopsis* requires the MYB75/PAP1 gene. Plant Physiology, 139: 1840–1852.

Voll L.M., Hajirezaei M.R., Czogalla-Peter C., Lein W., Stitt M., Sonnewald U., Frederik B. (2009): Antisense inhibition of enolase strongly limits the metabolism of aromatic amino acids, but has only minor effects on respiration in leaves of transgenic tobacco plants. New Phytologist, 184: 607–618.

Wu Z.J., Tian C., Jiang Q., Li X.H., Zhuang J. (2016): Selection of suitable reference genes for qRT-PCR normalization during leaf development and hormonal stimuli in tea plant (*Camellia sinensis*). Scientific Reports, 6: 19748.

Wang L.X., Pan D.Z., Liang M., Yakubu A., Jian L., Jinke L. (2017): Regulation of anthocyanin biosynthesis in purple leaves of Zijuan tea (*Camellia sinensis* var. Kitamura). International Journal of Molecular Sciences, 18: 833.

Wang Z.W., Jiang C., Wen Q., Wang N., Tao Y.Y., Xu L.A. (2014): Deep sequencing of the *Camellia chekiangoleosa* transcriptome revealed candidate genes for anthocyanin biosynthesis. Gene, 538: 1–7.

Ye J., Fang L., Zheng H. (2006): WEGO: A web tool for plotting GO annotations. Nucleic Acids Research, 34: W293–W297.

Zhao D.Q., Wei M.R., Liu D., Tao J. (2016): Anatomical and biochemical analysis reveal the role of anthocyanins in flower coloration of herbaceous peony. Plant Physiology and Biochemistry, 102: 97–106.

Zhao D., Jiang Y., Ning C., Meng J., Lin S., Ding W., Tao J. (2014): Transcriptome sequencing of a chimaera reveals coordinated expression of anthocyanin biosynthetic genes mediating yellow formation in herbaceous peony (*Paeonia lactiflora* Pall.). BMC Genomics, 15: 689.

Zhao M., Zhang D.L., Su X.Q., Duan S.M., Wan J.Q., Yuan W.X. (2015): An integrated metagenomics/metaproteomics investigation of the microbial communities and enzymes in solid-state fermentation of pu-erh tea. Scientific Reports, 5: 10117.

Zheng X.L., Tian S. (2006): Effect of oxalic acid on control of postharvest browning of litchi fruit. Food Chemistry, 96: 519–523.

Received: June 14, 2020
Accepted: April 6, 2022
Published online: May 17, 2022